OPEN CHARM PRODUCTION AT RHIC*

Zhangbu Xu

Physics Department, Brookhaven National Laboratory
Upton, NY 11973, USA

In this report, we present the measurements of open charm production at mid-rapidity in $p + p$, d+Au, and Au+Au collisions at RHIC energies. The techniques of direct reconstruction of open charm via its hadronic decay and indirect measurements via its semileptonic decay are discussed. The beam energy dependence of total charm cross section, electron p_{T} spectra, and their comparisons to theoretical calculations, including NLO pQCD, are presented. The electron spectra in $p + p$, d+Au, and Au+Au collisions at $\sqrt{s_{\mathrm{NN}}}$=200 GeV show significant variation. The open charm absolute cross section at midrapidity and its centrality dependence are compared to those of inclusive hadrons integrated over $p_{\mathrm{T}} > 1.5$ GeV/c.

PACS numbers: 25.27.Dw, 13.20.Fc, 13.25.Ft

1. Introductions

Hadrons with heavy flavor are unique tools for studying the strong interaction described by Quantum Chromodynamics (QCD). Due to the large charm quark mass, which requires large energies ($\gtrsim 3$ GeV) for their creation, charm quark production can be evaluated by perturbative QCD (pQCD) even at low momentum with the introduction of additional scales related to its mass [1, 2]. Therefore, the theoretical calculations of the charm hadron production cross section integrated over momentum space are expected to be less affected by non-perturbative processes and hadronization than those of the light hadrons [3]. Charm production has been proposed as a sensitive measurement of parton (gluon) distribution function in nucleon and the nuclear shadowing effect by systematical studies of $p + p$, and $p + A$ collisions [4]. The reduced energy loss of heavy quarks ("deadcone" effect) at momentum range $5 \lesssim p_{\mathrm{T}} \lesssim 10$ GeV/c will help us study the energy loss

---

* Presented at the XXXIV International Symposium on Multiparticle Dynamics, Sonoma County, California, USA, July 26–August 1, 2004.

mechanism within the partonic medium [5]. A possible enhancement of charmonium (J/ψ) production can be present at RHIC energies [6–9] through charm quark coalescence. This effect is opposed to the J/ψ suppression in a Quark–Gluon Plasma(QGP) in the absence of that process [10]. The measurement of both open charm yield and charmonia may allow us to quantify the effects and study whether charms are in chemical equilibrium with the system. In addition, the heavy flavor transverse momentum distributions and their anisotropic flow can be used to study the nature of early thermalization in $A + A$ collisions [11].

Identification of charmed hadrons is difficult due to its short lifetime ($c\tau(D^0) = 124$ μm), low production rate and overwhelming combinatoric background. Most measurements of the total charm cross section in hadron-hadron collisions were performed at low center-of-mass energies ($\lesssim 40$ GeV) in fixed target experiments [12, 13]. The measurements at high energy colliders were either at high p_T [14], with large uncertainty [15, 16] or inconsistency [17]. Theoretical predictions for RHIC energy region differ significantly [18, 19]. At RHIC, direct measurements of open charm from charm hadronic decays and indirect measurements from charm semileptonic decays in many beam conditions are possible. We will illustrate the techniques used in open charm measurements at RHIC and discuss the results.

2. Direct open charm reconstruction

The data used in D^0 direct reconstruction were taken during the 2003 RHIC run in d+Au collisions at $\sqrt{s_{\mathrm{NN}}}= 200$ GeV with the Solenoidal Tracker at RHIC (STAR) [20, 21]. A total of 15.7 million minimum bias triggered d+Au collision events were used in D^0 analysis. The primary tracking device of the STAR detector is the Time Projection Chamber (TPC) which was used to reconstruct the decay of $D^0 \rightarrow K^-\pi^+$ ($\overline{D^0} \rightarrow K^+\pi^-$) with a branching ratio of 3.83%. The invariant mass spectrum of $D^0(\overline{D^0})$ was obtained by pairing oppositely charged kaon and pion in same event with the parent rapidity $|y| < 1$. The kaon and pion tracks were identified through the ionization energy loss (dE/dx) in the TPC. The track reconstruction in the TPC gives a single track projection resolution of ~ 1cm around the collision vertex and therefore does not allow to resolve the exact decay topology. The D^0 signal in $p_T < 3$ GeV/c and $|y| < 1$ after mixed-event background subtraction [22] is shown in the left panel of Fig. 1.

In current STAR analyses, the total charm cross section is largely determined by directly reconstructed $D(\bar{D})$ at low p_T [20, 21]. In addition, D^* has been measured at $1.5 \lesssim p_T < 6$ GeV/c and $D^{\pm}, D^0$ at $p_T \simeq 10$ GeV/c [23]. In this presentation, we will focus on total charm cross section and its centrality dependence [20, 24].
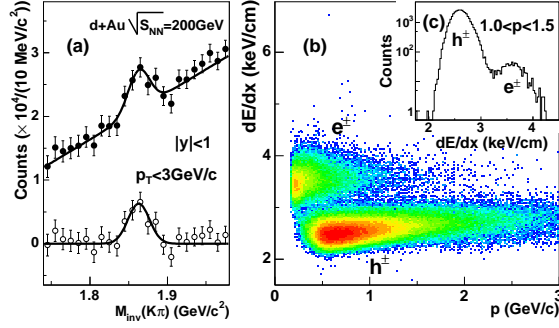
Fig. 1. (a) Invariant mass distributions of kaon–pion pairs from d+Au collisions. The solid circles depict signal after the mixed-event background subtraction, the open circles after subtraction of the residual background by a linear parameterization. (b) Ionization energy loss (dE/dx) in the TPC *vs* particle momentum (p) with a TOF cut of $|1/\beta - 1| \leq 0.03$. Insert: projection on the dE/dx axis for particle momenta $1 < p < 1.5$ GeV/c. Figure from [20].

3. Electron spectra from charm semileptonic decay

There are three techniques used to identify electrons in STAR and PHENIX:

1. **Tracking+RICH+EMCAL**
   This method is used by PHENIX collaboration to identify electrons [15,24]. Tracking from drift chamber and pad chamber provides particle track with high momentum resolution. A Ring Image Cerenkov Detector (RICH) is used as veto counter, and an electromagnetic calorimeter confirms the track's existence and provides a E/p measurement for electron selection.

2. **Tracking+dE/dx+EMC**
   This method is used by STAR collaboration to identify electron with $p \gtrsim 1.5$ GeV/c [20,21]. The STAR TPC not only provides tracking in a solenoidal field, but also has good particle identification capabilities through ionalization energy loss at resolution of about 8%. Due to relativistic rise of dE/dx of electron at high $\beta\gamma$, its separation from π, K and p are very good at hadron rejection of $> 10^{-2}$ at high p_T. The addition of $E/p = 1.0$ from EMC further reject π, K and p, and hadrons with high dE/dx (nuclei, ghost tracks). Since EMC can be used as a trigger detector, the electron spectra from this method can be extended to much higher p_T with high statistics [25].

3. **Tracking+dE/dx+TOF**
   This new technique is developed by STAR collaboration. A prototype time-of-flight system (TOFr) [26] based on the multi-gap resistive plate chamber technology was installed in STAR. It covers $-1 < \eta < 0$ and allows particle identification for $p_T < 3.5$ GeV/c. In addition to its capability of hadron identification [26], electrons could be identified at low momentum ($0.2 \lesssim p_T < 3$ GeV/c) by the combination of velocity (β) from TOFr and dE/dx from TPC measurements. The right panel of Fig. 1 demonstrates the clean separation of electrons from hadrons using their energy loss (dE/dx) in the TPC after applying a TOFr cut of $|1/\beta - 1| \leq 0.03$. This cut eliminated the hadrons crossing the electron dE/dx band. Electrons were required to originate from the primary vertex. Hadron contamination was evaluated to be about 10–15% in this selection.

Gamma conversions $\gamma \rightarrow e^+e^-$ and $\pi^0 \rightarrow \gamma e^+e^-$ Dalitz decays are the dominant photonic sources of electron background. There are again several methods used to study the background electron sources:

1. **Cocktail modeling**
   This method was adapted by PHENIX Collaboration in their first publication [15]. The cocktail is a detailed detector simulation of electrons/positrons from γ conversion and Dalitz decays from π^0, η and other photonic sources.

2. **Converter**
   This method was adapted by PHENIX Collaboration in their latest report [24]. Two datasets with and without a converter with known thickness were taken and analyzed. The two measurements allows to untangle the sources associated with photon conversion and those without. Species-dependent Dalitz fraction per γ and contribution from other photonic sources (η, ω, ρ, ϕ and K) are evaluated by detailed detector simulations.

3. **Invariant mass reconstruction**
   The e^+e^- pairs from photon conversions and Dalitz decays are present mainly at small pair invariant mass and/or small opening angle [20,21]. Due to the large coverage of the TPC, the efficiency of finding pairs is very high for such processes. To measure the background, the invariant mass and opening angle of the pairs were constructed by first selecting an electron (positron) in TOFr and then matching it with every positron (electron) candidate reconstructed in the TPC [27] without additional requirement of a secondary vertex at the conversion point.

In this method, both inclusive electron spectra and background sources are taken from same dataset, and the reconstructed background spectrum is not sensitive to the detailed knowledge of the conversion and Dalitz decay. About 95% of electrons from sources other than charm semileptonic decays have been measured with this method, while the remaining fraction ($< 5\%$) from decays of η, ω, ρ, ϕ and K was determined from detailed detector simulations.

4. Discussions

Fig. 2 shows the energy dependence of the electron p_T spectra from ISR to Tevatron. Direct open charm measurements (STAR, CDF) are converted to electron spectra. Several measurements at RHIC have shown to be consistent between (dE/dx+EMC), direct $\boldsymbol{D}$, (dE/dx+TOF) [21,23,25] at STAR, and to some extent, the measurements in $p+p$ collisions between STAR and PHENIX [28]. Fig. 2 shows significant dispersion of electron distribution at
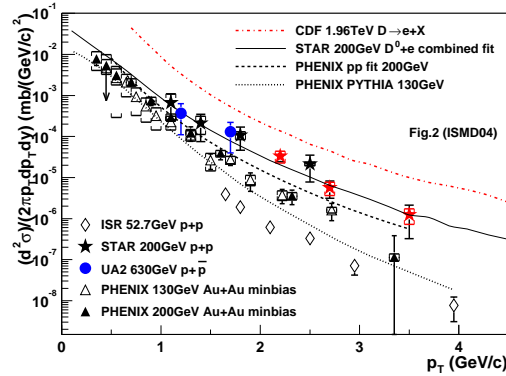

Fig. 2. Non-photonic electron p_T distributions from $p+p$, $p+\bar{p}$, d+Au, and Au+Au at different beam energies from ISR to Tevatron.

$\sqrt{s_{\mathrm{NN}}}$=200 GeV at RHIC from Au+Au, d+Au to $p+p$ at $p_T \simeq 2$ GeV/c where statistics are still high. The variation in spectra is possibly due to the interactions between the charm quark (hadron) and the medium [29]. The deadcone effect [5] would be most effective at $5 \lesssim p_T \lesssim 10$ GeV/c and not yet accessible at the p_T range ($\simeq 2$ GeV/c) of electrons. The beam energy dependence of the cross section is shown in Fig. 3. The PHENIX results are derived from electron spectrum in Au+Au minbias collisions using the electron spectrum shape from PYTHIA6.205 [24]. The STAR result is from a combined fit of D^0 and electron spectra in d+Au minbias collisions. At $\sqrt{s} \sim 52$–63 GeV, the available measurements are inconclusive due to the inconsistency between different measurements [12] and are omitted. At
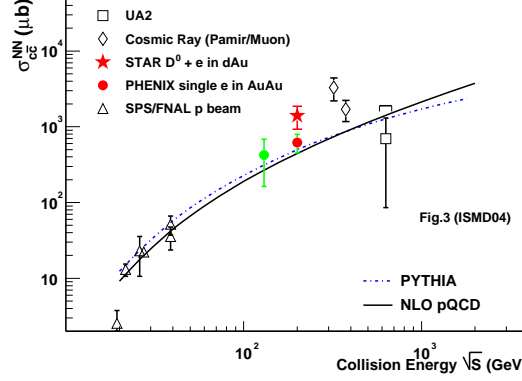
Fig. 3. Total $c\bar{c}$ cross section per nucleon–nucleon collision *vs* the collision energy (in $\sqrt{s_{\rm NN}}$).

$\sqrt{s_{NN}} = 200$ GeV, both PYTHIA and NLO pQCD calculations underpredict the total charm cross section [18, 30]. This is evident from STAR data but less pronounced in PHENIX results. There are indications that a large charm production cross section ($\sigma_{c\bar{c}}^{NN} \simeq 2$–3 mb) at $\sqrt{s_{NN}} \simeq 300$ GeV is essential to explain cosmic ray data [31]. The centrality dependence of charm $d\sigma/dy$ per binary nucleon–nucleon collision at midrapidity shows possible dependence on centrality with lower production cross section in central collisions as in Fig. 4. In the same figure, the cross sections per binary nucleon–nucleon
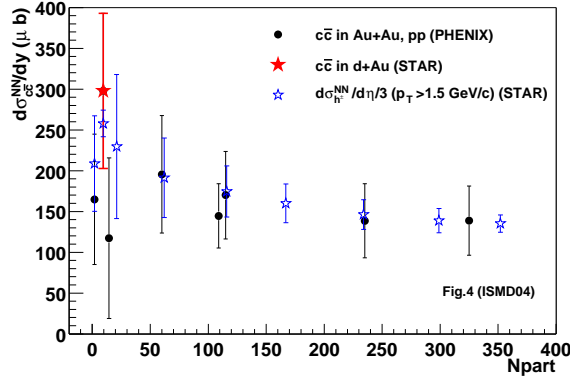

Fig. 4.   Charm differential cross section per binary nucleon–nucleon collision ($d\sigma_{c\bar{c}}^{NN}/dy$) at midrapidity as function of number of participant nucleons at RHIC $\sqrt{s_{\rm NN}}$=200 GeV. Also plotted as open stars are cross section per binary nucleon–nucleon collisions ($d\sigma_{h\pm}^{NN}/d\eta$ (μb)) of inclusive hadrons integrated over $p_{\rm T} > 1.5$ GeV/c ($\simeq m_D$) and scaled down by a factor of three.

collisions of inclusive hadrons [32] $(d\sigma_{h^\pm}/d\eta/3(\mu b))$, which were integrated over $p_T > 1.5$ GeV/c (close to the mass of charm hadron m_D) and scaled down by a factor of 3 for three light quark flavors, show same magnitude of absolute cross section and a similar trend. This may suggest that particle production rate is not sensitive to flavor when the momentum transfer is above the production threshold. We note that final state interactions in $A + A$ collisions may affect the hadron yields above $p_T > 1.5$ GeV/c.

A direct reconstruction of open charm spectra in Au+Au collisions from $0 \lesssim p_T \lesssim 10$ GeV/c in future runs, when compared with those from d+Au data [20,23], will enable us to study the thermalization at low p_T and deadcone effect at high p_T. The elliptic flow v_2 measurements of charm flow with higher statistics at the same p_T range will further strengthen the case, since early thermalization will result in large v_2 at low p_T, and absence of large energy loss due to deadcone effect may result in smaller v_2 at high p_T when compared to those of light hadrons.

5. Summary

In summary, charm cross section and transverse momentum distributions from $p + p$, d+Au and Au+Au collisions have been measured by the STAR and PHENIX collaborations at RHIC. The NLO calculation underpredicts the total cross section in this energy range. A possible centrality dependence of charm cross section can explain the marginally different cross sections observed by STAR in d+Au collisions and PHENIX in Au+Au collisions. We look forward to more results using charm as probe to the hot and dense medium created at RHIC from run4 and future runs.

REFERENCES

[1] P.L. McGaughey *et al.*, *Int. J. Mod. Phys.* **A10**, 2999 (1995).

[2] M.L. Mangano *et al.*, *Nucl. Phys.* **B405**, 507 (1993).

[3] S.S. Adler *et al.*, (PHENIX Collaboration), *Phys. Rev. Lett.* **91**, 241803 (2003); J. Adams *et al.*, (STAR Collaboration), *Phys. Rev. Lett.* **92**, 171801 (2004).

[4] Z. Lin, M. Gyulassy, *Phys. Rev. Lett.* **77**, 1222 (1996).

[5] Y.L. Dokshitzer, D.E. Kharzeev, *Phys. Lett.* **B519**, 199 (2001).

[6] A. Andronic *et al.*, *Phys. Lett.* **B571**, 36 (2003), and references therein.

[7] R.L. Thews, M. Schroedter, J. Rafelski, *Phys. Rev.* **C63**, 054905 (2001), and references therein.

[8] L. Grandchamp, R. Rapp, *Phys. Lett.* **B523**, 60 (2001).

[9] M.I. Gorenstein *et al.*, *J. Phys. G* **28**, 2151 (2002).

[10] T. Matsui, H. Satz, *Phys. Lett.* **B178**, 416 (1986).

[11] N. Xu, Z. Xu, *Nucl. Phys.* **A715**, 587c (2003); S. Batsouli *et al.*, *Phys. Lett.* **B 557**, 26 (2003); Z.W. Lin, D. Molnar, *Phys. Rev.* **C 68**, 044901 (2003); X. Dong *et al.*, *Phys. Lett.* **B597**, 328 (2004).

[12] S.P.K. Tavernier, *Rep. Prog. Phys.* **50**, 1439 (1987), and references therein.

[13] G.A. Alves *et al.*, (E769 Collaboration), *Phys. Rev. Lett.* **77**, 2388 (1996).

[14] D. Acosta *et al.*, (CDF II Collaboration), *Phys. Rev. Lett.* **94**, 241804 (2003).

[15] K. Adcox *et al.*, (PHENIX Collaboration), *Phys. Rev. Lett.* **88**, 192303 (2002).

[16] O. Botner *et al.*, (UA2 Collaboration), *Phys. Lett.* **B236**, 488 (1990).

[17] F.W. Büsser *et al.*, *Nucl. Phys.* **B113**, 189 (1976).

[18] R. Vogt, `hep-ph/0203151`, and references therein. The curve in Fig. 3 is a NLO pQCD calculation with CTEQ5M, $\mu_{\mathrm{F}} = \mu_{\mathrm{R}} = 2m_c$, $m_c = 1.2$ GeV/c^2.

[19] J. Raufeisen, J.-C. Peng, *Phys. Rev.* **D67**, 054008 (2003).

[20] J. Adams *et al.* (STAR Collaboration), `nucl-ex/0407006`.

[21] L.J. Ruan, *J. Phys. G* **30**, S1197 (2004) [`nucl-ex/0403054`]; H. Zhang, DNP 2003, Hot Quarks 2004.

[22] C. Adler *et al.*, *Phys. Rev.* **C66**, 06190(R) (2002); H. Zhang, *J. Phys. G* **30**, S577 (2004).

[23] A. Tai, *J. Phys. G* **30**, S809 (2004) [`nucl-ex/0404029`].

[24] PHENIX Collaboration, S.S. Adler *et al.*, `nucl-ex/0409028`.

[25] A.A.P. Suaide, *J. Phys. G* **30**, S1179 (2004) [`nucl-ex/0404019`].

[26] J. Adams *et al.*, (STAR Collaboration), `nucl-ex/0309012`.

[27] J. Adams *et al.*, (STAR Collaboration), *Phys. Rev.* **C70**, 044902 (2004) [`nucl-ex/0401008`].

[28] R. Averbeck, *J. Phys. G* **30**, S943 (2004).

[29] D. Teaney, BNL seminar; private communications.

[30] T. Sjöstrand, L. Lönnblad, S. Mrenna, `hep-ph/0108264`. In this paper we used PYTHIA 6.152 with CTEQ5M1.

[31] I.V. Rakobolskaya *et al.*, *Nucl. Phys.* **B112**, 353c (2003).

[32] J. Adams *et al.*, (STAR Collaboration), *Phys. Rev. Lett.* **91**, 172302 (2003); *Phys. Rev. Lett.* **91**, 072304 (2003).